Endothelial protein C–targeting liposomes show enhanced uptake and improved therapeutic efficacy in human retinal endothelial cells

Arta, Anthoula; Eriksen, Anne Z.; Melander, Fredrik; Kempen, Paul; Larsen, Michael; Andresen, Thomas L.; Urquhart, Andrew J.

Published in:
Investigative Ophthalmology and Visual Science

DOI:
10.1167/iovs.18-23800

Publication date:
2018

Document version
Publisher's PDF, also known as Version of record

Endothelial Protein C–Targeting Liposomes Show Enhanced Uptake and Improved Therapeutic Efficacy in Human Retinal Endothelial Cells

Anthoula Arta,[1] Anne Z. Eriksen,[1] Fredrik Melander,[1] Paul Kempen,[1] Michael Larsen,[2,3] Thomas L. Andresen,[1] and Andrew J. Urquhart[1]

[1]Department for Micro- and Nanotechnology, Technical University of Denmark, Kongens Lyngby, Denmark
[2]Department of Ophthalmology, Rigshospitalet, Glostrup, Denmark
[3]Faculty of Health and Medical Sciences, University of Copenhagen, Copenhagen, Denmark

Correspondence: Andrew J. Urquhart, Department for Micro- and Nanotechnology, Technical University of Denmark, 2800 Kongens Lyngby, Denmark; anur@nanotech.dtu.dk.

Submitted: January 6, 2018
Accepted: March 19, 2018

Citation: Arta A, Eriksen AZ, Melander F, et al. Endothelial protein C–targeting liposomes show enhanced uptake and improved therapeutic efficacy in human retinal endothelial cells. *Invest Ophthalmol Vis Sci*. 2018;59:2119–2132. https://doi.org/10.1167/iovs.18-23800

Purpose. To determine whether human retinal endothelial cells (HRECs) express the endothelial cell protein C receptor (EPCR) and to realize its potential as a targeting moiety by developing novel single and dual corticosteroid–loaded functionalized liposomes that exhibit both enhanced uptake by HRECs and superior biologic activity compared to nontargeting liposomes and free drug.

Methods. EPCR expression of HRECs was investigated through flow cytometry and Western blot assays. EPCR-targeting liposomes were developed by functionalizing EPCR-specific antibodies onto liposomes, and the uptake of liposomes was assessed with flow cytometry and confocal laser scanning microscopy. The therapeutic potential of EPCR-targeting liposomes was determined by loading them with prednisolone either through bilayer insertion and/or by remote loading into the aqueous core. The carrier efficacy was assessed in two ways through its ability to inhibit secretion of interleukins in cells stimulated with high glucose and angiogenesis in vitro by using an endothelial cell tube formation assay.

Results. HRECs express EPCR at a similar level in both human aortic and umbilic vein endothelial cells. The EPCR-targeting liposomes displayed at least a 3-fold higher uptake compared to nontargeting liposomes. This enhanced uptake was translated into superior anti-inflammatory efficacy, as the corticosteroid-loaded EPCR-targeting liposomes significantly reduced the secretion of IL-8 and IL-6 and inhibited the development of cell tube formations in contrast to nontargeting liposomes.

Conclusions. We show that HRECs express EPCR and this receptor could be a promising nanomedicine target in ocular diseases where the endothelial barrier of the retina is compromised.

Keywords: retina, liposomes, EPCR, corticosteroids, endothelial cells

Diabetic retinopathy is the most common microvascular implication of diabetes mellitus and corresponds to the leading cause of visual impairment in adults between 20 and 65 years old in the developed world.[1,2] Its hallmark features include weakening of tight junctions, formation of microaneurysms on the retinal capillaries, pericyte loss, endothelial cell loss, retinal ischemia with secondary preretinal neovascularization, capillary leakage, and macular edema.[3–5] Breakdown of the blood-retina barrier in diabetic retinopathy is a characteristic feature of the more severe levels of retinopathy that may provide a special opportunity to deliver drugs to the endothelium and other components of the retina, be it from the luminal or abluminal side of the vessel wall. The exposed endothelium presents an opportunity for targeted drug delivery at the site of disease.

Endothelial cell protein C receptor (EPCR/CD201) is a transmembrane glycoprotein that facilitates the activation of protein C and thereby regulates the anticoagulation pathway.[6,7] It has been shown to be a critical for life receptor, if its expression is knocked down or compromised due to pathologic reasons.[8–10] A soluble form, produced by metalloprotease cleavage from the cell membrane,[11] works along with the membrane-bound EPCR in the pathophysiology of sepsis and inflammation in a poorly understood manner.[6,12] EPCR was initially thought to be expressed only on the endothelium of large vessels but was then found on smooth muscle cells, neutrophils, keratinocytes, and microvascular endothelia such as that of the brain capillaries.[13–15] To the best of our knowledge, it has not previously been identified on human retinal endothelial cells (HRECs).

In this study, we investigated the expression of EPCR on HRECs and the potential of this receptor as a target for drug nanocarriers by using unilamellar liposomes as a model system. Liposomes, uni- or multi-lamellar vesicles comprised of phospholipids and, frequently, cholesterol, have a range of attractive properties as drug carriers, including ease of assembly, low cytotoxicity, and a high loading capacity for both hydrophobic and hydrophilic drugs.[16,17] Liposomes have a history of clinical approval[18] and have demonstrated promising intraocular results (e.g., sustained drug release, high therapeu-

tic efficacy, and reduced cytotoxicity of the drugs).[19,20] Here, we report EPCR expression on HRECs in comparison to human aortic endothelial cells (HAECs) and human umbilical vein endothelial cells (HUVECs). We determined the targeting efficiency of functionalized liposomes with EPCR-specific monoclonal antibodies on HRECs and HAECs. Furthermore, we assessed the anti-inflammatory efficacy of EPCR-targeting liposomes when loaded with the corticosteroid prednisolone (either prednisolone 21-hemisuccinate sodium salt [PH] and/or prednisolone 21-palmitate [PP]) through the inhibition of IL-8 and IL-1β and IL-6 expression in stimulated HRECs, as well as the ability to inhibit angiogenesis in vitro using an endothelial cell tube formation assay.

Materials and Methods

Materials

Cholesterol (Chol), 1,2-dipalmitoyl-sn-glycero-3-phosphocholine (DPPC), 1,2-distearoyl-sn-glycero-3-phosphoethanolamine-N-(methoxy[polyethylene glycol]-2000) (PEG) and 1,2-distearoyl-sn-glycero-3-phosphoethanolamine-N-(maleimide[polyethylene glycol]-2000) (maleimide) were all purchased from Avanti Polar Lipids (Alabaster, AL, USA). 1,2-dipalmitoyl-sn-glycero-3-phosphoethanolamine-N-lissamine (DPPE-Atto) was purchased from Atto-TEC (Siegen, Germany). Prednisolone, PH, mannitol, HEPES, NaCl, N,N′-dicyclohexylcarbodiimide, 4-(dimethylamino)pyridine, palmitic acid, and all organic solvents were purchased from Sigma-Aldrich Corp. (St. Louis, MO, USA). ELISA kits for IL-1β, IL-6, and IL-8, along with the Human Cytokine Array kit were obtained from R&D Systems Inc. (Minneapolis, MN, USA), and the Matrigel matrix was purchased from Corning (Flintshire, UK). The monoclonal antibodies Alexa Fluor 488 rat anti-human CD201 clone RCR-252, Alexa Fluor 488 rat IgG1 κ isotype control clone R3-34, and rat anti-human CD201 clone RCR-252 (anti/EPCR) were purchased from BD Biosciences (San Jose, CA, USA).

PP Synthesis, Purification, and Characterization

The synthesis of PP was achieved using Steglich esterification. Prednisolone, palmitic acid, N,N′-dicyclohexylcarbodiimide, and 4-(dimethylamino)pyridine (1:1:2:2 molar ratio) were all dissolved in excess dichloromethane under an N_2 atmosphere and left stirring at room temperature for 18 hours. The reaction was followed by thin-layer chromatography using a chloroform:methanol (95:5) mobile phase. PP appeared as a streaked spot close to the baseline. Dichloromethane was evaporated under rotation and reduced pressure to leave a crude product. Crude product was redissolved in a chloroform:methanol (95:5) mixture and purified on a silica gel column by using a chloroform:methanol (95:5) mobile phase. The resulting purified PP had a high yield (>85%) and high purity (>97%). Purity was determined by both analytic high pressure liquid chromatography (HPLC) and ^{1}H nuclear magnetic resonance (NMR) spectroscopy. ^{1}H NMR ($CHCl_3$-D) key characteristic peaks include the following: δ 0.88 (t, 3H, 37), 0.98 (s, 3H, 18), 1.25 (s, 24H, 25–36), 1.45 (s, 3H, 19), 4.48 (m, 1H, 11), 4.87 (d, 1H, J = 17.4 Hz, 21), 4.97 (d, 1H, J = 17.4 Hz, 21), 6.00 (t, 1H, 4), 6.27 (dd, J = 10.09, 1.89 Hz, 2), and 7.27 (d, J = 10.1 Hz, 1). The remaining corticosteroid ring ^{1}H chemical shifts followed similar values (e.g., δ 1.6–2.6 covers protons at 6, 7, 8, 12, 14, 15, 16, and 23) as previously reported for prednisolone, similar corticosteroids, and functionalized corticosteroids where functionalization occurred at position 21 (see Supplementary Fig. S1 for ^{1}H NMR spectrum and atom numbering).[21–23]

Liposome Preparation and Loading

All liposomes were prepared by mixing the lipids in a tertiary butanol:water (9:1) mixture and lyophilized overnight in a Christ Epsilon 2-4 LSCplus freeze dryer (Buch & Holm, Herlev, Danmark). Subsequently the lipid mixtures were rehydrated with 10 mM HEPES saline buffer or with a 200 mM calcium acetate buffer (Sigma-Aldrich Corp.) for the remote loading of PH. Lipid suspensions were prepared at 15 mM and hydrated at 60°C with gentle vortexing for 60 minutes, followed by extrusion through a 100-nm filter at 60°C.[24] For the liposome formulations with membrane-loaded PP, the extrusion was performed in 3 steps through 400-nm, 200-nm, and finally through 100-nm filters. Remote loading was performed using a protocol previously described.[25,26] Briefly, the liposomes were subjected to 3 repeated 1-hour dialysis cycles by using a ratio of liposome dispersion to dialyzing medium (5% glucose) 1:200, followed by a forth dialysis step overnight of 1:400. PH was dissolved in 5% glucose and was mixed with liposomes in a drug to lipid ratio of 1:2. Remote loading was achieved by incubation of the liposomes with the drug for 20 minutes at 60 to 65°C, with continuous stirring. Nonencapsulated drug was removed by 2-step dialysis (dialysis tubing, MWCO 10 kDa; Sigma-Aldrich Corp.) using a ratio of 1:500 sample to diluent (10 mM HEPES, pH 7.4, 150 mM NaCl), with the first step lasting for 4 hours at 4°C and the second step overnight at 4°C. For the uptake studies, the different systems that we prepared were of the following molar ratios: (1) DPPC/Chol/PEG/maleimide/DPPE-Atto, 55.92:40:3:1:0.08, (2) DPPC/Chol/DPPE-Atto, 59.92:40:0.08, and (3) DPPC/Chol/PEG/DPPE-Atto, 55.92:40:4:0.08. For the flow cytometry experiments, DPPE-Atto 655 was used and for the microscopy images, DPPE-Atto 488 was used. We did not observe any size or charge differences of the liposomal carriers when replacing fluorophores. For the efficacy studies, we removed fluorophore-conjugated phospholipids so the formulations for these experiments were DPPC/Chol/ PEG/maleimide (56:40:3:1) and DPPC/Chol/PEG (56:40:4), and we included an extra formulation of DPPC/Chol/ PEG/maleimide/PP (51:40:3:1:5) with a 5% molar concentration of PP in the bilayer. See Tables 1 and 2 for all liposome formulations.

Liposome Characterization

The diameter and surface charge of the liposomes were measured on a Brookhaven ZetaPALS zeta potential analyzer (New York, NY, USA) as previously described.[27] Briefly, diameters (measured by dynamic light scattering) and zeta potentials were measured in 10 mM HEPES in a 5% glucose solution. Phospholipid concentrations were determined by quantifying the phosphorous content in the liposome samples by using inductively coupled plasma mass spectrometry. For further confirmation of the liposome size distribution measured by dynamic light scattering, we used Cryo-transmission electron microscopy (TEM). For each experiment, 3 μL of lipid dispersions at a concentration of 3 mM was placed on a lacy carbon 300 mesh copper TEM grid, blotted and plunge frozen in liquid ethane by using a FEI Vitrobot Mark IV (Thermo Fisher Scientific, OR, USA). Samples were transferred to the TEM at −175°C by using a Gatan 626 single tilt cryo-transfer holder (Gatan, Inc., Pleasanton, CA, United States) and were imaged using a FEI Tecnai G2 20 TWIN TEM operated at 200 keV in low dose mode with a FEI high-sensitive 4k × 4k Eagle camera. The loading of both PH and PP was quantified by reverse phase HPLC, and the loading efficiency was calculated by the drug-to-lipid ratios before and after purification.

Investigative Ophthalmology & Visual Science

Table 1. Liposome Formulations and Characteristics Used in the Uptake Studies

Formulations	Abbreviation	Size, nm	PDI	Zeta Potential, mV
DPPC:Chol:PEG:DPPE-Atto (55.92:40:4:0.08)	P-NL	157.5 ± 1.4	0.03 ± 0.02	−17.84 ± 0.85
DPPC:Chol:DPPE-Atto (59.92:40:0.08)	B-NL	153.1 ± 0.9	0.07 ± 0.01	−0.96 ± 2.1
DPPC:Chol:PEG:maleimide:DPPE-Atto-anti/EPCR (55.92:40:3:1:0.08)	EPCR-NL	162.5 ± 1.4	0.02 ± 0.01	−16.09 ± 1.62
DPPC:Chol:PEG:maleimide:DPPE-Atto-isotype (55.92:40:3:1:0.08)	Iso-NL	161.3 ± 1.7	0.07 ± 0.03	−14.21 ± 1.17

Liposome Functionalization

Rat anti-human CD201 clone RCR-252 and isotype IgG control (rat IgG1; BD Biosciences) antibodies were diluted to a final concentration of 0.45 mg/mL in 0.2 M sodium borate buffer (pH 8.5) mixed with 2-iminothiolane (Traut's reagent; Sigma-Aldrich Corp.) at a molar ratio of 1:20. The thiolation reaction proceeded for 60 minutes at room temperature, and the thiolated antibodies were then transferred to Amicon Ultra 4-mL spin filters (MWCO 30 kDa; Merck Life Science, Søborg, Denmark). The spin filters were filled with cold 10 mM HEPES buffer and centrifuged at 2500*g* for 30 minutes at 4°C. This process was repeated 2 times to purify the thiolated antibodies from unreacted 2-iminothiolane. The thiolated antibodies were immediately mixed with DSPE-PEG-maleimide liposomes in a molar ratio of 10:1 (of the available maleimide groups) and the liposome-antibody mixture was incubated overnight on a rocking table (180 rpm) in the dark to allow for conjugation.[28,29] After the incubation, the antibody-functionalized liposomes were separated from the nonbound antibodies by size-exclusion chromatography using a Sepharose CL-4B column (Sigma-Aldrich, Corp.) with a 10 mM HEPES, 150 mM NaCl (pH 7.4) buffer as the fluid phase. The size-exclusion chromatography fractions were analyzed by the BCA assay (Thermo Fisher Scientific, Hvidovre, DK) for the antibody concentration, and the fractions containing antibody-functionalized liposomes were up-concentrated using Amicon Ultra 4-mL spin filters (MWCO 30 kDa; Merck Life Science) at 2500*g* and at 4°C.

Release Profile In Vitro

The dialysis method was used to characterize the in vitro release behavior of the PH-loaded liposomes. We loaded 1 mL of 6 mM liposomes into dialysis bag (MWCO 10 kDa) and incubated them in 9 mL of 10 mM HEPES saline buffer at 37°C with continuous stirring for 120 hours. At predetermined timepoints, 200 µL of release media was sampled and equal volumes of fresh media was added. The cumulative release of PH was calculated after analyzing the samples by HPLC ($n = 4$).

Cell Culture

HRECs were purchased from Innoprot (Bizkaia, Spain), and the HAECs and HUVECs were purchased from LGC Standards GmbH (Wesel, Germany). The cells were grown to 85 to 90% confluency in the endothelial cell medium (Innoprot) supplemented with 5% (vol/vol) fetal bovine serum, 1% (vol/vol) penicillin/streptomycin in an environment of 95% O_2 and 5% CO_2. For the endothelial cell tube formation assay, the cells were cultured on Matrigel matrix (Corning). 96-well plates were coated with Matrigel (50 µL/well) at 4°C and were incubated at 37°C for 30 minutes. Subsequently, 15×10^3 HRECs were seeded in each well with a final volume of 200 µL endothelial cell medium.

Cell Viability (MTS Assay)

Cell proliferation and viability were evaluated by an MTS assay. HRECs, HAECs, and HUVECs were seeded into 96-well plates at a density of 3×10^3 cells per well per 100 µL. Twenty-four hours later, the cells were exposed to PH at concentrations from 1 nM to 1 mM for 4 hours. The cells were incubated for 48 hours and then 20 µL MTS reagent was added to each well. The absorbance at 490 nm was measured by a microplate reader 4 hours later. The same process was followed in order to determine the cytotoxicity of our liposomal system. The cells were incubated with liposomes at lipid concentrations from 100 nM to 500 µM.

Detection of EPCR in HRECs by Flow Cytometry and Western Blot

In order to determine whether HRECs express EPCR or not, we used flow cytometry and Western blot assays. For the flow cytometry, HRECs, HAECs, and HUVECs were seeded in T75 flasks (Thermo Scientific) and grown to 85 to 90% confluency in the endothelial cell medium (Innoprot) supplemented with 5% (vol/vol) fetal bovine serum and 1% (vol/vol) penicillin/streptomycin in an environment of 95% O_2 and 5% CO_2. When the cells reached confluency, they were washed in PBS, 3 mL of trypsin-EDTA was then added to each flask, and flasks were incubated for 5 minutes. The cell suspensions were centrifuged (200*g*, 20°C, 5 minutes), the collected cell pellet was resuspended in cold PBS, and this process was repeated once more. The washes were collected in Eppendorf (Hørsholm, Denmark) tubes with a concentration of 5×10^5 cells per tube per 500 µL of PBS. Cells were then incubated with 10 µg/mL of Alexa Fluor 488 rat anti-human CD201 clone RCR-252 or Alexa Fluor 488 rat IgG1 κ isotype control clone R3-34 for 30 minutes at 4°C (BD Biosciences). The cell suspensions were washed twice with PBS, were transferred to flow cytometry tubes, and analyzed using a BD Accuri C6 autosampler flow cytometer (BD Biosciences). In each experiment, 20,000 events were analyzed and at least 3 independent experiments were performed.

For the Western blot assay, the HRECs and the HAECs were seeded in T25 flasks (Thermo Scientific) and grown to 85 to

Table 2. Liposome Formulations and Characteristics Used for the Efficacy Studies

Formulations	Abbreviation	Size, nm	PDI	Zeta Potential, mV
DPPC:Chol:PEG (56:40:4) + PH	P-NL1	149.5 ± 1.1	0.04 ± 0.03	−16.82 ± 1.12
DPPC:Chol:PEG:maleimide-anti/EPCR (56:40:3:1) + PH	EPCR-NL1	162.7 ± 0.9	0.05 ± 0.03	−14.19 ± 1.32
PP:DPPC:Chol:PEG:maleimide-anti/EPCR (5:51:40:3:1) + PH	EPCR-NL2	101.2 ± 1.3	0.03 ± 0.01	−15.49 ± 1.71
DPPC:Chol:PEG:maleimide-anti/EPCR (56:40:3:1)	EPCR-NL	160.3 ± 1.5	0.03 ± 0.02	−15.93 ± 1.65

90% confluency. For transfection, when cells reached 70 to 80% confluency, they were incubated with EPCR/PROCR silencer predesigned siRNA (Thermo Fisher Scientific) Lipofectamine 2000 (Thermo Fisher Scientific) complexes. Briefly, 500 pmol of siRNA was diluted in 250 μL Opti-MEM I reduced serum medium and 5 μL Lipofectamine 2000 was diluted in 250 μL of Opti-MEM I reduced serum medium, and both solutions were incubated for 15 minutes at room temperature. After the 15 minute incubation, the diluted siRNA and the diluted Lipofectamine 2000 were combined and incubated for 15 minutes at room temperature so as to allow complexes to form. Subsequently, the siRNA-Lipofectamine 2000 complexes were added to the T25 flasks at a total of 5 mL medium and incubated at 37°C in a humidified CO_2 incubator for 24 hours. Then, the cells were washed 2 times with cold PBS, lysed with lysis buffer (25 mM Tris-HCl; pH, 7.4; 0.15 M NaCl; 1% Triton X-100) with complete Mini Protease Inhibitor Cocktail (Sigma-Aldrich Corp.) and Phosphatase Inhibitor Cocktail 2 (Sigma-Aldrich Corp.), then placed on a shaker at 4°C for 30 minutes. After centrifugation at 12,000*g* for 10 minutes, the protein concentration of the supernatant was measured by BCA assay (Thermo Fisher Scientific). Subsequently, equal amounts of 20 μg of protein were loaded and separated by 4 to 12% Bis-Tris gel electrophoresis (Thermo Fisher Scientific). The proteins were transferred to a nitrocellulose membrane (Thermo Fisher Scientific). Following the transfer, the immunoblot was incubated with Odyssey blocking buffer (LI-COR Biosciences, Cambridg, UK) at room temperature for 1 hour with agitation. EPCR was detected by monoclonal rat anti-EPCR/CD201 antibody (RCR-252) (Abcam, Cambridge, UK) at 1:50 dilution in which the membrane was incubated overnight at 4°C. The membrane was washed 3 times by tris-buffered saline and Tween 20 for 5 minutes, and then the second antibody (goat anti-rat IgG [H+L] Cross-Adsorbed Secondary Antibody, DyLight 800; Thermo Fisher Scientific), at 1:10,000 dilution, was incubated at room temperature for 1 hour. The membrane was washed 3 times with tris-buffered saline and Tween 20, and the protein bands were visualized by Odyssey Fc Imaging System (LI-COR Biosciences).

Quantification of Liposome Uptake by Cells Using Flow Cytometry

We evaluated the uptake of fluorescently labeled liposomes by endothelial cells with flow cytometry. HRECs, HAECs, and HUVECs were seeded at a density of 12×10^5 cells per well in 12-well plates (Thermo Scientific) in 1 mL of the culture medium at 37°C under an atmosphere with 5% CO_2. After 24 hours, the cells were incubated with the Atto 655–labeled carriers at a liposomal concentration of 75 μM in medium for 1 hour, 2 hours, or 3 hours. For the experiments where we blocked EPCR, we added 5 μg of rat anti-human CD201 clone RCR-252 in each well and incubated for 20 minutes. Then, we added the liposomes without washing off the antibody. Subsequently, the cells were washed with PBS and then trypsinized. The cell suspension was centrifuged (200*g*, 20°C, 5 minutes), and then the collected cells were resuspended in 1 mL PBS. The latter process was repeated 3 times, and then the cells were transferred to flow cytometry tubes and analyzed using the Gallios flow cytometer (Beckman-Coulter, Copenhagen, DK). Cells were gated based on the forward/side scatter plot to eliminate cell debris from the subsequent analysis. At least 10,000 events were analyzed in each experiment and a minimum of three independent experiments were performed. The fluorescence intensity of the liposome treated cells was corrected based on the autofluorescence of nontreated cells and the resulting data was analyzed using FlowJo software (FlowJo LLC, Oregon, USA).

Confocal Laser Scanning Microscopy

Further estimation of the uptake of the different carriers was performed by confocal laser scanning microscopy. In that case, 25×10^3 cells were seeded in a μ-Slide 8 well (ibidi GmbH, Planegg, Germany) in 300 μL of culture medium as a 2D culture or on Matrigel matrix. After 24 hours, the cells were incubated with 75 μM of the different Atto 488–labeled carriers for 3.5 hours. Subsequently, 20 mL of TO-PRO-3 (1 μM; Thermo Fisher Scientific) dye was added to stain the nuclei, and the suspension was reincubated for an additional 30 minutes. The medium was then removed, and the cells were washed twice with 300 μL PBS, before they were fixed with 4% paraformaldehyde for 10 minutes at room temperature and washed again twice with 300 μL of PBS. After fixation, and only for the 2D cultured cells, 300 μL of Phalloidin-TRITC in 10 mM HEPES (1:300; Sigma-Aldrich) was added to each well and incubated for 1 hour at room temperature. Eventually, each well was washed twice with PBS, and confocal imaging was performed using a Leica TC SP5 confocal laser scanning microscope (Leica Microsystems GmbH, Wetzlar, Germany).

Stimulation of Cells by High Glucose and Cytokine Quantification

To study the anti-inflammatory efficacy of our carrier, we stimulated an inflammatory response in the cells by culturing them in high glucose conditions. For these studies, only the primary cell lines were used. HRECs and HAECs were seeded in 12-well plates at a concentration of 30×10^3 cells/well under either normal glucose (5.5 mM), mannitol (20 mM, mannitol-osmolarity control), or high glucose (25 mM) conditions for up to 3 days. Twenty-four hours after having been seeded in high glucose, the cells were treated with the following: (1) 25 μM prednisolone hemisuccinate in the form of free drug, (2) 25 μM prednisolone hemisuccinate encapsulated in the targeting liposomal system, with or without PreP on the membrane, or (3) 25 μM prednisolone hemisuccinate encapsulated in nontargeting liposomes (P-NL) for 4 hours, then washed and incubated at 37°C with 5% CO_2. Subsequently, we collected the cell supernatant 24 hours following the treatment, centrifuged them at 3000*g* for 5 minutes, and saved the samples at −80°C. New medium was added to the wells and incubated at 37°C with 5% CO_2 for another 24 hours when we again collected the supernatant, 48 hours after treatment. Concentrations of IL-1β, IL-8, and IL-6 protein in culture supernatant were determined using an ELISA.

Endothelial Cell Tube Formation Assay

Angiogenesis was studied by assessment of tube formation on HRECs seeded onto Matrigel matrix (Corning), as has been previously described.[30] After coating the 96-well plates with Matrigel, 15×10^3 HRECs were seeded in each well with a final volume of 200 μL. To determine the effect of the drug and the liposomes on the capillary tube formation, HRECs were incubated under 6 different conditions from the onset of the culture: (1) no treatment (control), (2) empty liposomes, (3) 50 μM prednisolone hemisuccinate as free drug, (4) 50 μM prednisolone hemisuccinate encapsulated in the targeting liposomal system, with or without PP, or (5) 50 μM prednisolone hemisuccinate in nontargeting liposomes. Phase-contrast images (5× magnification) of the center of each well were taken 4 hours, 8 hours, and 24 hours after seeding the cells, and tube formation was quantified using the Angiogenesis Analyzer tool for ImageJ (reported as the total length of the tubelike formations and the number of segments formed) (National Institutes of Health, Bethesda, MA, USA).

Investigative Ophthalmology & Visual Science

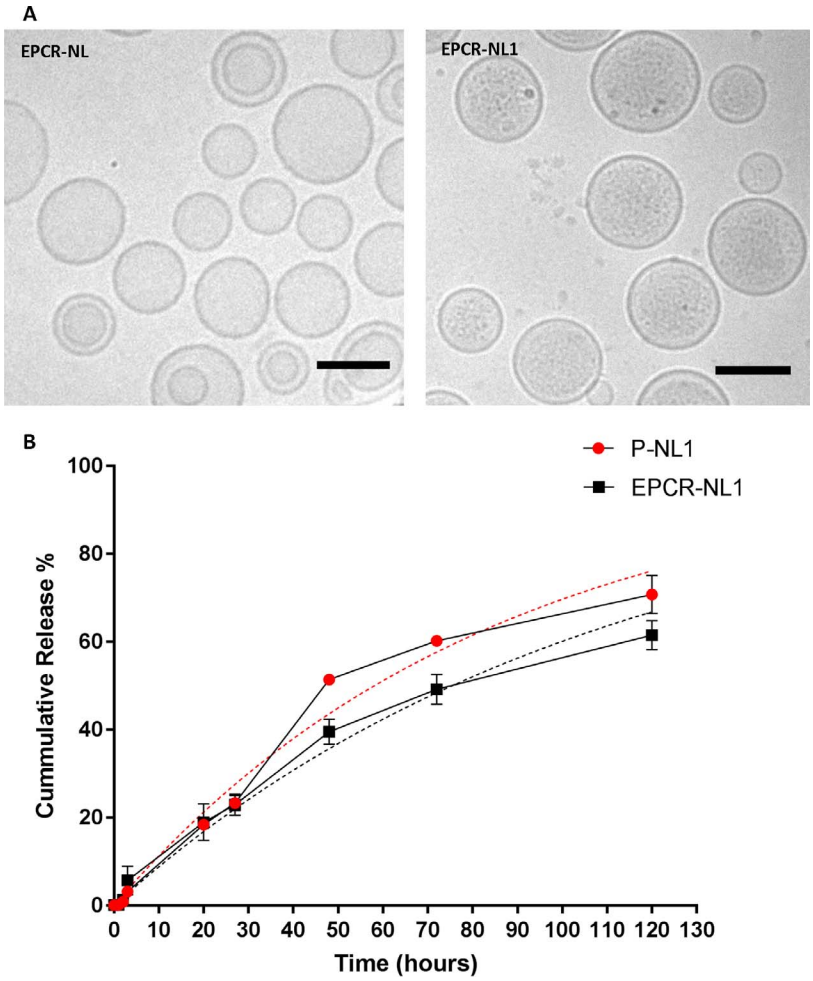

FIGURE 1. Liposome characteristics. (**A**) Cryo-TEM image of nonloaded (EPCR-NL) and PH-loaded EPCR-targeting (EPCR-NL1) liposomes. *Scale bar*: 100 nm. (**B**) Cumulative PH release profile of EPCR-NL1 and P-NL1 liposomes. The *dashed lines* represent first order fits of each release profile.

Cell Experiment Statistics

Data were expressed as mean ± SEM and a one-way ANOVA with a confidence level of 95% ($\alpha = 0.05$), followed by a Tukey's multiple comparison post hoc test ($P < 0.05$) were used in order to analyze significant differences in the in vitro assays.

RESULTS

Characterization of Liposomes

Size distribution, polydispersity index (PDI), and zeta-potential were measured for each formulation (see Tables 1 and 2), and the structure of the empty and loaded liposomes was further characterized by cryo-TEM imaging (Fig. 1A). Liposome formulations without PP had diameters ranging from 150 to 165 nm, and from the cryo-TEM images, it was observed that most of the liposomes were unilamellar and spherical in shape. The precipitation of PH in the core of the liposomes was also observed. The formulation with PP had slightly smaller diameters of approximately 100 nm. The loading efficiency for PP was 45% (± 3.2%), whereas for PH was 70% (± 2.8%). Moreover, the cumulative release profile of PH for both antibody functionalized and nonfunctionalized liposomes showed sustained release for 5 days without any initial burst, but with a slightly higher release rate for the nonfunctionalized liposomes compared to the EPCR-targeting ones (Fig. 1B). PH release profiles from targeting and nontargeting liposomes could be fitted best with a first order exponential (P-NL1, $R^2 = 0.969$; EPCR-NL1, $R^2 = 0.947$), which indicates that the release rate of drug is dependent on the drug concentration.[31]

EPCR Expression in HRECs

In order to determine whether or not HRECs express EPCR, we selected 2 endothelial cell types (HUVECs and HAECs[7]) that have already shown strong expression of the receptor, and we compared all 3 with flow cytometry. From the analysis of these experiments, we observed a shift of 2 orders of magnitude in the median fluorescent intensity (MFI) levels of the HRECs that were incubated with the anti-EPCR monoclonal antibody, compared to the isotype-treated cells or the nontreated ones. This shift was similar to shifts observed for HAECs and HUVECs, which can be approximated as 99.9% of HRECs expressing EPCR at similar levels to the other 2 endothelial cell lines (Fig. 2A). See Supplementary Fig. S2 for fluorescence-activated cell sorting scatter plots.

The comparison between HRECs and HAECs through Western blots indicated similar immunoblotting for both endothelial cell types at 49 kDa and 38 kDa (Fig. 2B). The double band can be explained by the fact that EPCR has 4 N-linked glycosylation sites that can be heterogeneously modified, which results in a glycosylated mass of ≤49 kDa that

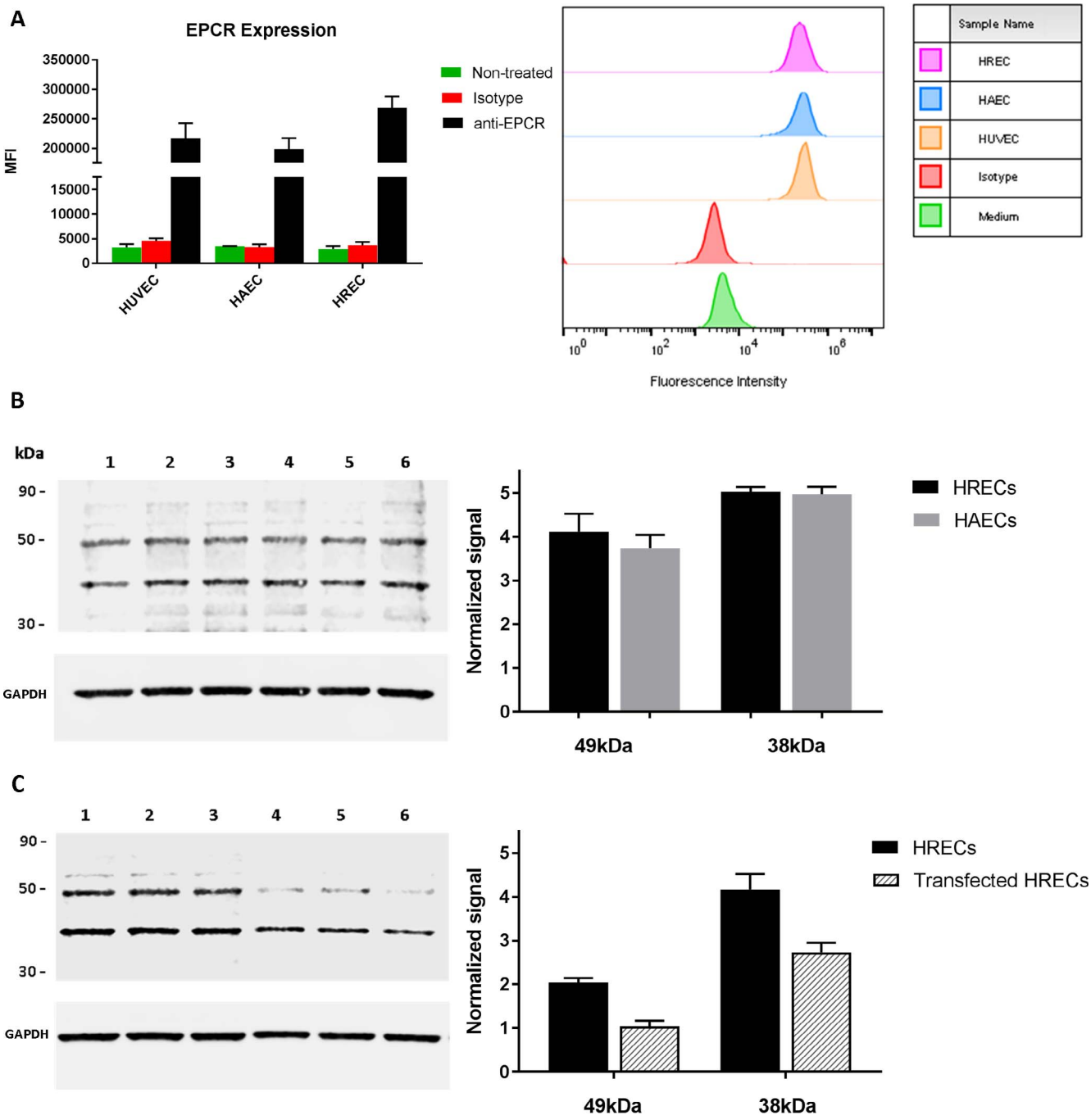

Figure 2. EPCR expression in endothelial cells. (**A**) Flow cytometry analysis of EPCR expression in HRECs. Cells were incubated with isotype control IgG or anti–EPCR monoclonal antibody (RCR-252), both conjugated with Alexa Fluor 488, and the autofluorescence of the cells is indicated from the nontreated ones. EPCR expression estimated by MFI determined by flow cytometry analysis from 3 independent experiments is shown on the *left*, and example flow cytometry histograms from 1 of the experiments on the *right*. (**B**) Immunoblotting of cell surface EPCR by RCR-252. Western blot (*left*) where lanes 1–3 represent HRECs and lanes 4–6 represent HAECs. Densitometry of Western blot data is show on the *right*. (**C**) Western blot (*left*) where lanes 1–3 represent HRECs and lanes 4–6 represent transfected HRECs with EPCR knockdown siRNA. Densitometry of this is shown on the *right*.

varies among cell lines.[32] As another approach to confirm the cell surface expression of EPCR from HRECs, we transfected HRECs with EPCR knockdown siRNA and immunoblotted the total protein extract (~20 μg) of both transfected and nontransfected HRECs. In this case, we can see strong binding of the anti-EPCR monoclonal antibody at 49 kDa and 38 kDa for HRECs cells, but for the transfected cells, there is a 2-fold reduction at the normalized signal of the 49 kDa band and a noticeable decrease at the 38 kDa band (Fig. 2C).

EPCR-Targeting Effects on Cellular Uptake

Once we had established the expression of EPCR on the surface of HRECs, we investigated the potential of targeting this receptor with antibody-functionalized liposomes. For the

first set of experiments, liposomes functionalized with either the EPCR-specific antibody or isotype were incubated for 4 hours with cells. As a second negative control, EPCR was blocked by incubating the cells with the monoclonal anti-EPCR antibody before adding the EPCR-targeting liposomes. EPCR-targeting liposomes associated strongly with both HRECs and HAECs, which corresponded to an 8.3-fold increase in the MFI compared to isotype IgG liposomes and a 5.2-fold increase compared to the cells with the blocked receptor (Fig. 3A). Subsequently, we wanted to compare the binding and uptake of the EPCR-targeting liposomes with other nontargeting liposomes, so we made nonfunctionalized/blank (B-NL) and P-NL liposome formulations. We then performed a time study in order to investigate how uptake evolves with different incubation times. Analysis of the flow cytometry data showed that the EPCR-targeting liposomes (EPCR-NL) displayed significantly higher uptake with the HRECs and HUVECs after 1 hour of incubation (Fig. 3B) than P-NL (3.2-fold) and B-NL (5.7-fold). The results for HAECs were similar, with EPCR-NL being higher than P-NL (2.3-fold) and B-NL (4.6-fold). Furthermore, we found that the longer the incubation time, the higher the uptake by cells with all the different formulations. However, EPCR-NL repeatedly showed more than 3-fold higher MFI compared to P-NL after 2 hours and 3 hours of incubation with HRECS and more than 6-fold higher than B-NL. Similar behavior was observed for HAECs and HUVECs. HAECs showed 2-fold higher uptake of EPCR-NL than P-NL after both 2-hour and 3-hour incubations, whereas a 4-fold higher uptake of EPCR-NL was observed compared to B-NL. HUVECs showed a more than a 3-fold higher MFI for EPCR-NL compared to the P-NL formulation (2-hour and 3-hour incubations) and >5.5-fold higher compared with the B-NL one (Fig. 3B). All results showed statistical significance with P values generally below 0.01.

The strong interaction between EPCR-targeting liposomes and the HRECs could also be visualized by confocal laser scanning microscopy. From Z-stack projections, we were able to detect strong fluorescent signal from the EPCR-targeting liposomes, mainly in the intracellular compartment of the HRECs (Fig. 4). In agreement with the flow cytometry results, the signal from the HRECs that were incubated with the P-NL formulation was much weaker (Fig. 4B) and in the case of the B-NL, no signal was detected (Fig. 4C).

Reduction of ILs by Corticosteroid-Loaded EPCR-Targeting Liposomes

To assess whether the enhanced uptake of EPCR-targeting liposomes by endothelial cells resulted in an improved therapeutic efficacy, we exposed HRECs and HAECs to corticosteroid-loaded liposomes, PH loaded EPCR-NL1 and dual-loaded (PP and PH) EPCR-NL2, and measured changes in IL levels. We first stimulated increased IL expression in HRECs and HAECs by culturing them in high glucose conditions. We then tested the changes in the secretion levels of 3 different inflammatory mediators with or without corticosteroid treatment. IL-6 and IL-8 levels were significantly increased under high glucose conditions for both HRECs and HAECs compared to normal glucose conditions. The latter inflammatory effect was significantly suppressed when the cells were treated with free PH or PH encapsulated in the EPCR-targeting liposomes (EPCR-NL1) (Fig. 5). According to the PH release profiles from the liposomes, after 24 hours, less than 23% (22.5 ± 3.4 % at 26 hours) of PH had been released, whereas at 48 hours, approximately 40% (39.2 ± 3.9 % at 48 hours) PH release had occurred. This corresponds to 6 μM of PH released from the EPCR-NL1 liposomes in 24 hours, followed by 4 μM released over the next 24 hours (i.e., ∼5 μM per day). EPCR-NL1 liposomes induced a similar anti-inflammatory effect, releasing 5 μM per day compared to the single 25-μM dose of free PH. Single doses of free PH at 10 μM showed no effect on reducing IL-6 and IL-8 levels in HRECs over 48 hours (see Supplementary Fig. S4).

The dual-loaded (PP and PH) EPCR-targeting liposome (EPCR-NL2) exhibited superior performance to EPCR-NL1 in HRECs, indicating that PP was actively contributing to IL reduction even though lipid anchored and at concentrations (∼2.4 μM) significantly lower than PH (∼25 μM) in the liposomes. For HRECs that were treated with EPCR-NL1, we observed a 35% decrease in the IL-8 secretion both in day 1 and day 2 after treatment. For EPCR-NL2, there was a 45% decrease after day 1 and a 40% decrease after day 2. For IL-6, a 25% decrease was observed for EPCR-NL1 after day 1 and day 2, whereas for EPCR-NL2, this corresponded to a 42 and 39% decrease (Fig. 5A). The PH loaded PEG surface-functionalized nontargeting liposome P-NL1 exhibited significantly poorer performance than both EPCR-NL1 and EPCR-NL2; more specifically, a less than 15% decrease was observed for IL-6, whereas no significant reduction in the IL-8 secretion was observed (Fig. 5A). The difference between the formulations can be attributed to the 3-fold lower uptake of P-NL compared to EPCR-NL for HRECs (Fig. 3). Moreover, the performance of the EPCR-NL1 compared to the nontargeting but drug loaded liposomes was considerably better, with a 30% reduction in IL-8 secretion both 1 and 2 days after treatment. The EPCR-NL2 formulation performed significantly better than either EPCR-NL1 ($P < 0.001$) or the free drug ($P < 0.01$). HAECs responded in a similar manner (Fig. 5B) with EPCR-NL1 inducing a 35% decrease in the IL-8 secretion after day 1 and 37% after day 2, whereas for EPCR-NL2, this was 40 and 45%. IL-6 secretion was also inhibited with either EPCR-NL1 (20% and 25% decrease for day 1 and day 2, respectively) or EPCR-NL2 treatment (30% and 25% decrease for day 1 and day 2, respectively). The P-NL1 formulation displayed inferior performance compared to the EPCR-targeting formulation or the free PH but a better performance than P-NL1 in HRECs. This likely reflects the better uptake of P-NL by HAECs than HRECs (Fig. 3). We did not observe similar behavior for IL-1β and were not able to detect any difference in IL-1β secretion levels for any of the 5 different conditions for HRECs or HAECs (data not shown).

Inhibition of In Vitro Angiogenesis by Corticosteroid-Loaded EPCR-targeting liposomes

In another attempt to explore the potential efficacy of targeting EPCR, we tested the ability of EPCR-NL1 to inhibit angiogenesis in vitro in an endothelial cell tube formation assay. Before the efficacy studies, we tested the uptake of our liposomes by HRECs in tube-like formations on Matrigel matrix. The results were similar to what we previously observed from the uptake studies in monolayer culture conditions; more specifically, we detected strong fluorescent signal from EPCR-NL1, but weaker signal from P-NL and no signal from B-NL (Fig. 6A–D). The ability of HRECs to form tube-like structures was estimated by calculating the number of segments and the total length of the tube formations from images taken 8 hours after seeding the cells on Matrigel. Incubating the cells with EPCR-NL1 and EPCR-NL2 liposomes significantly inhibited tube-like formations compared to untreated cells, as shown by the decrease in the total tube length ($P < 0.05$) and the number of segments ($P < 0.05$ and $P < 0.01$) (Fig. 6E, 6F). Using the PH release profiles (Fig. 1B) at 8 hours, we extrapolated that 7.8% of PH has been released by ECPR-NL, corresponding to 3.9 μM. This is significantly lower than the 50 μM of free PH required to induce a similar effect on both tube length and the number of segments (Fig. 6E, 6F). We did not observe any reduction in

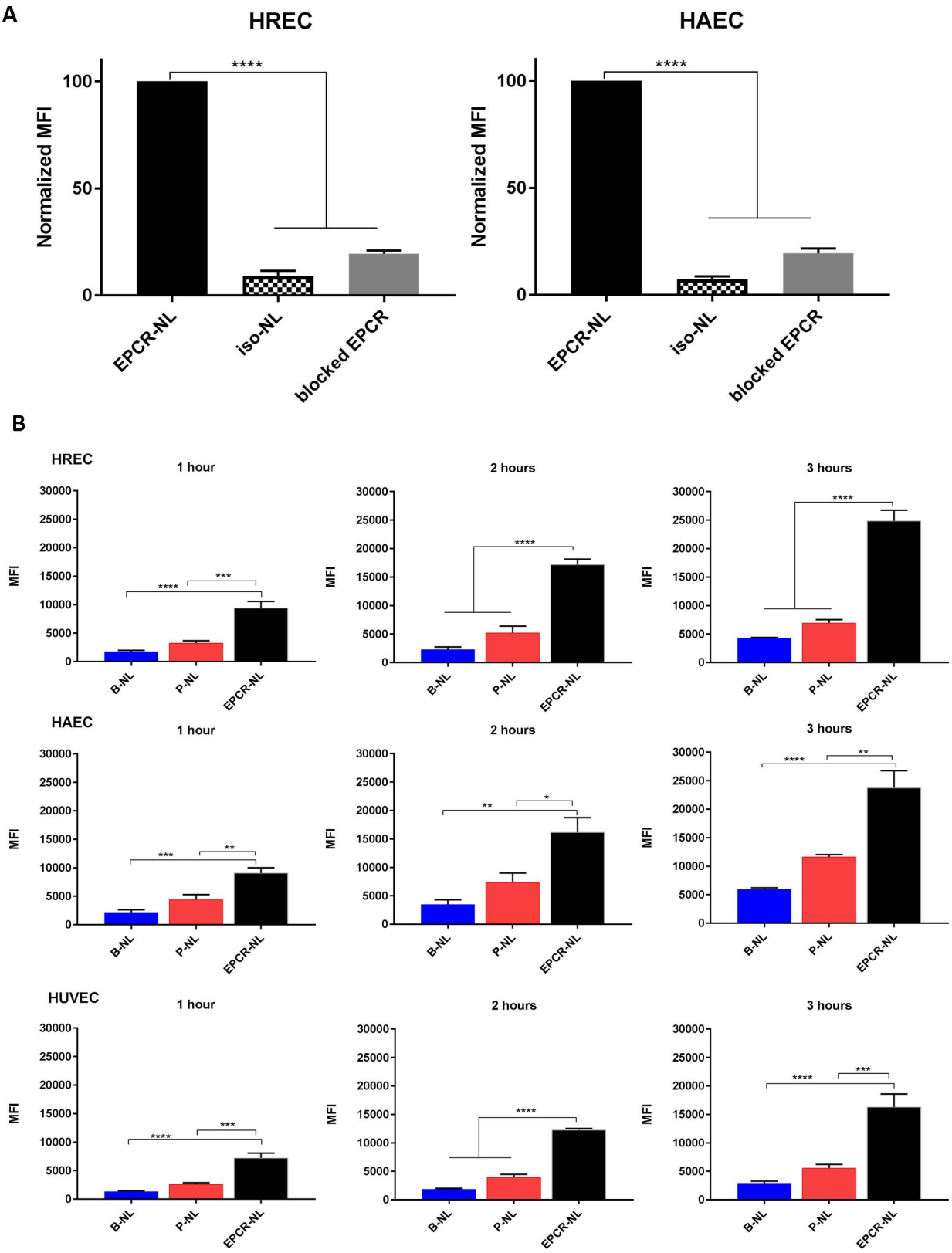

FIGURE 3. Flow cytometry evalution of liposome uptake in endothelial cells. (**A**) Flow cytometry evaluation of the association between EPCR-targeting liposomes and endothelial cells. HRECs and HAECs were incubated with either EPCR-targeting liposomes (EPCR-NL), isotype IgG functionalized liposomes (Iso-NL), or with EPCR-specific antibody (blocked EPCR) before adding the EPCR-targeting liposomes in order to block the receptor. All MFI values are normalized to the MFI of the EPCR-NL. (**B**) Flow cytometry assessment of the liposome uptake by endothelial cells. HRECS, HAECs, and HUVECs were incubated with either EPCR-NL, P-NL, or B-NL liposomes for 3 different incubation times: 1 hour, 2 hour, or 3 hour. $^{**}P < 0.01$, $^{***}P < 0.001$, $^{****}P < 0.0001$.

Investigative Ophthalmology & Visual Science

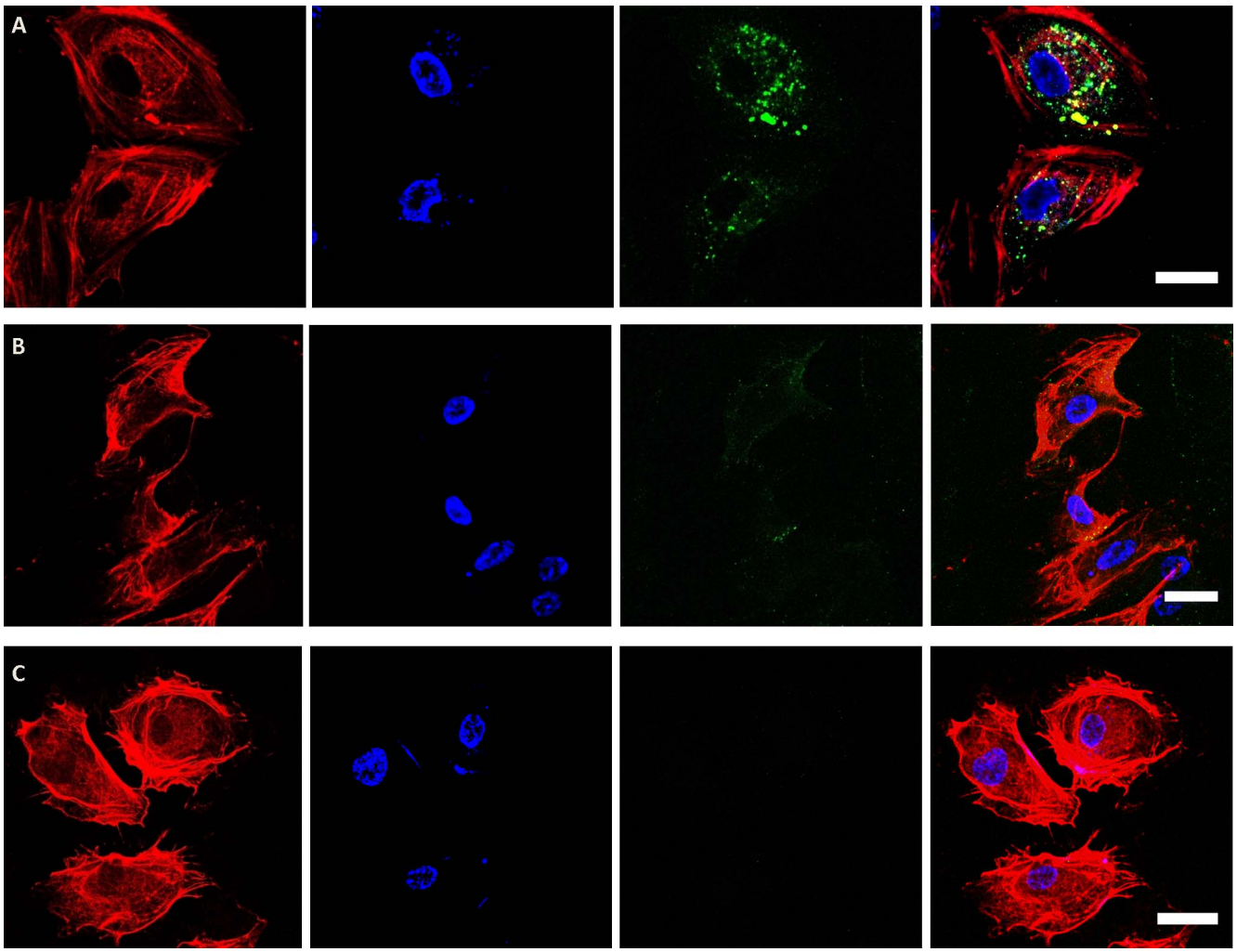

FIGURE 4. Confocal laser scanning microscopy of EPCR-targeting liposomes and HRECs: (**A**) HRECs incubated with EPCR-NL liposomes, (**B**) HRECs incubated with P-NL liposomes, (**C**) HRECs incubated with B-NL liposomes. The first column shows actin staining (Phalloidin-TRITC), the second column shows nucleus staining (TO-PRO-3), the third column shows liposomes (Atto 488), and the fourth column shows columns 1–3 merged. *Scale bar*: 25 μm.

tube length or the number of segments at 25 μM of free PH (data not shown). Furthermore, P-NL1 treatment did not induce any significant reduction in tube length or the number of segments, even though PH release is similar to EPCR-NL (7.9%). This indicates that the enhanced uptake of EPCR-targeting liposomes leads to the improved efficacy of prednisolone.

DISCUSSION

In this study, we showed for the first time that EPCR is expressed by HRECs. It has been previously shown through histologic studies in humans and baboons that all large vessels and arteries express high levels of EPCR. In the brain microvasculature, which can be used as direct comparison to the retina, the expression was lower.[14] The latter observation provides a strong argument that EPCR should be expressed in the human retinal endothelium as well. In an attempt to realize the level of EPCR expression, we performed a comparative study between HRECs and 2 other endothelial cell types, HEACs and HUVECs, which have been shown to heavily express the receptor in vitro.[7] The flow cytometry and immunoblotting assays indicated similar levels of EPCR expression in all 3 different cell types, leading to the conclusion that HRECs strongly express EPCR in vitro.

In order to investigate the potential of EPCR as a nanomedicine target, we functionalized EPCR-specific antibody onto the surface of liposomes to study the uptake of these liposomes by HRECs, HAECs, and HUVECs in comparison to 2 nontargeting formulations. All of our formulations used saturated lipids (DPPC and DPPE-Atto), which, due to higher transition temperatures compared to unsaturated lipids, tend to exhibit better stability.[33] In our case with P-NL formulations, we obtained a sustained PH release for up to 5 days, which was not the case for unsaturated formulations that exhibited burst release within the first 24 hours (data not shown). We also incorporated cholesterol into all of our formulations, as it has been previously shown that adding 30 to 40 mol% of cholesterol can significantly improve the stability of liposomes.[34,35] Functionalizing the surface of the liposomes with PEG is a widely used technique in order to not only improve the circulation/residency time of nanocarriers[34] but also to improve nanocarrier mobility in the vitreous.[36,37] We chose to PEGylate our EPCR-targeting formulation due to the benefits of PEG, but we also used a formulation with no surface

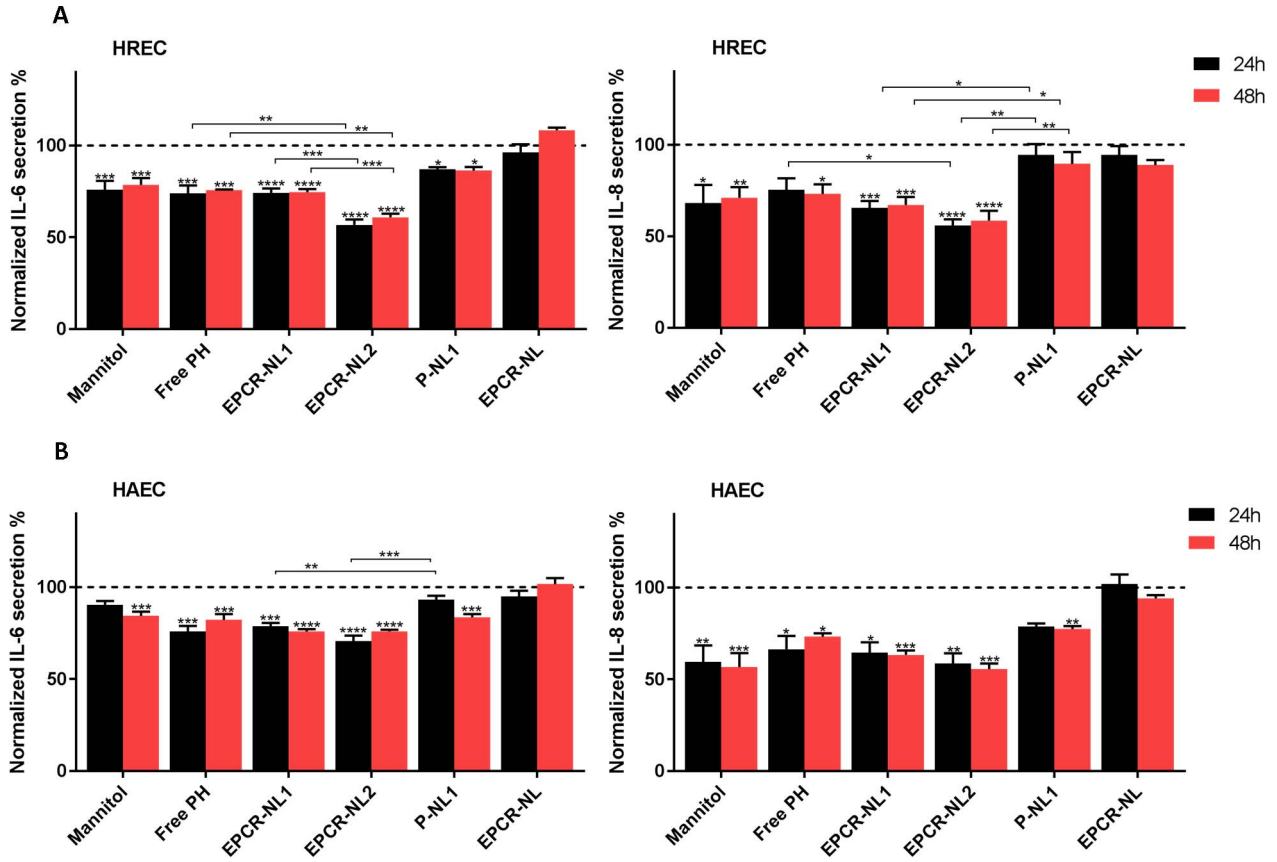

Figure 5. Secretion of IL-6 and IL-8 from endothelial cells normalized to the values of the untreated cells cultured under high glucose conditions (*dashed line*). (**A**) Effect of free or loaded PH on HRECs. (**B**) Effect of free or loaded PH on HAECs. In both cases (HRECs and HAECs) cells were exposed to free PH (25 μM) or PH loaded into either EPCR-targeting liposomes (EPCR-NL1), EPCR-targeting liposomes with PP in the membrane (EPCR-NL2), or nontargeting liposomes (P-NL1). The cells were subjected to the different treatments for 4 hours, then washed, and supernatants were collected 24 hours and 48 hour after the exposure. At the 24-hour timepoint, all liposomes had released ~6 μM of PH, whereas at 48 hours all liposomes had released an additional ~4 μM (i.e., ~10 μM cumulative) of PH. All IL expression was normalized to cells cultured under high glucose (*dashed line*). Cells cultured in 20 mM mannitol to represent healthy cells or stimulated cells treated with empty liposomes (EPCR-NL) were used as controls. The significance levels are $^{*}P < 0.05$, $^{**}P < 0.01$, $^{***}P < 0.001$, $^{****}P < 0.0001$.

functionalization (B-NL) to investigate how PEGylation would affect the uptake of the liposomes by the cells.

In all the experiments, the EPCR-targeting liposomes displayed significantly higher uptake than the control formulations, even for incubation times as short as 1 hour. In order to establish that it was actually EPCR-targeting that lead to the enhanced uptake, EPCR was blocked before incubating with the EPCR-targeting liposomes. This blockage lead to a 5-fold inhibition of the uptake of the carrier with both HRECs and HAECs ($P < 0.0001$), clearly indicating that EPCR targeting drove the enhanced uptake.

The delivery of corticosteroid drugs to the posterior part of the eye is a challenge because systemic administration is associated with undesirable systemic side effects and eye drop formulations have poor penetration. In contrast, injection of corticosteroid into the vitreous is very effective in controlling inflammation and macular edema secondary to diabetic retinopathy and retinal vein occlusion. Diabetic retinopathy is closely linked to hyperglycemia, low-grade chronic inflammation, and elevated reactive oxygen species[3,38,39] and is dominated by the development of microaneurysms, hemorrhage, vascular leakage, macular edema, and preretinal neovascularization at the back of the eye.[3,4] Several studies have indicated that there is a significant increase in the levels of proangiogenic and proinflammatory factors and cytokines (e.g., vascular endothelial growth factor, IL-8, TNF-α, IL-6, and IL-1β) in the vitreous of a patient with diabetic retinopathy.[40–43] These findings have led to the emergence of several novel treatment modalities based on the administration of antivascular endothelial growth factor agents and corticosteroids to the diseased retina.[44,45] Corticosteroids are an attractive option due to their broad range of actions including anti-inflammatory and antiangiogenic effects.[46–49] Corticosteroid-loaded liposomes have been reported for several decades, but drug loading efficacy and release rates have presented significant challenges. The passive loading of hydrophilic corticosteroids in liposomes initially resulted in very low encapsulation efficiencies (<5%).[50–52] Low loading can be overcome by choosing amphipathic weak acid corticosteroids and using a remote-loading approach. It has been shown that using a calcium acetate ion gradient can lead to high loading efficiencies of corticosteroid succinates, with 80% encapsulation efficiency (EE) for betamethasone hemisuccinate, 100% EE for hydrocortisone hemisuccinate, and 95% EE for methylprednisolone hemisuccinate.[25,52] In our case, we achieved a 70% EE for PH that is lower compared to the other corticosteroids, and this could likely be improved by optimizing the loading parameters. Furthermore, palmitate corticosteroid derivatives have also been studied since the late 1970s, with cortisol palmitate, prednisolone palmitate, and dexamethasone palmitate having been loaded into liposomes.[53–55] In our case, we loaded 5% molar concentration of PP into our liposomes with a

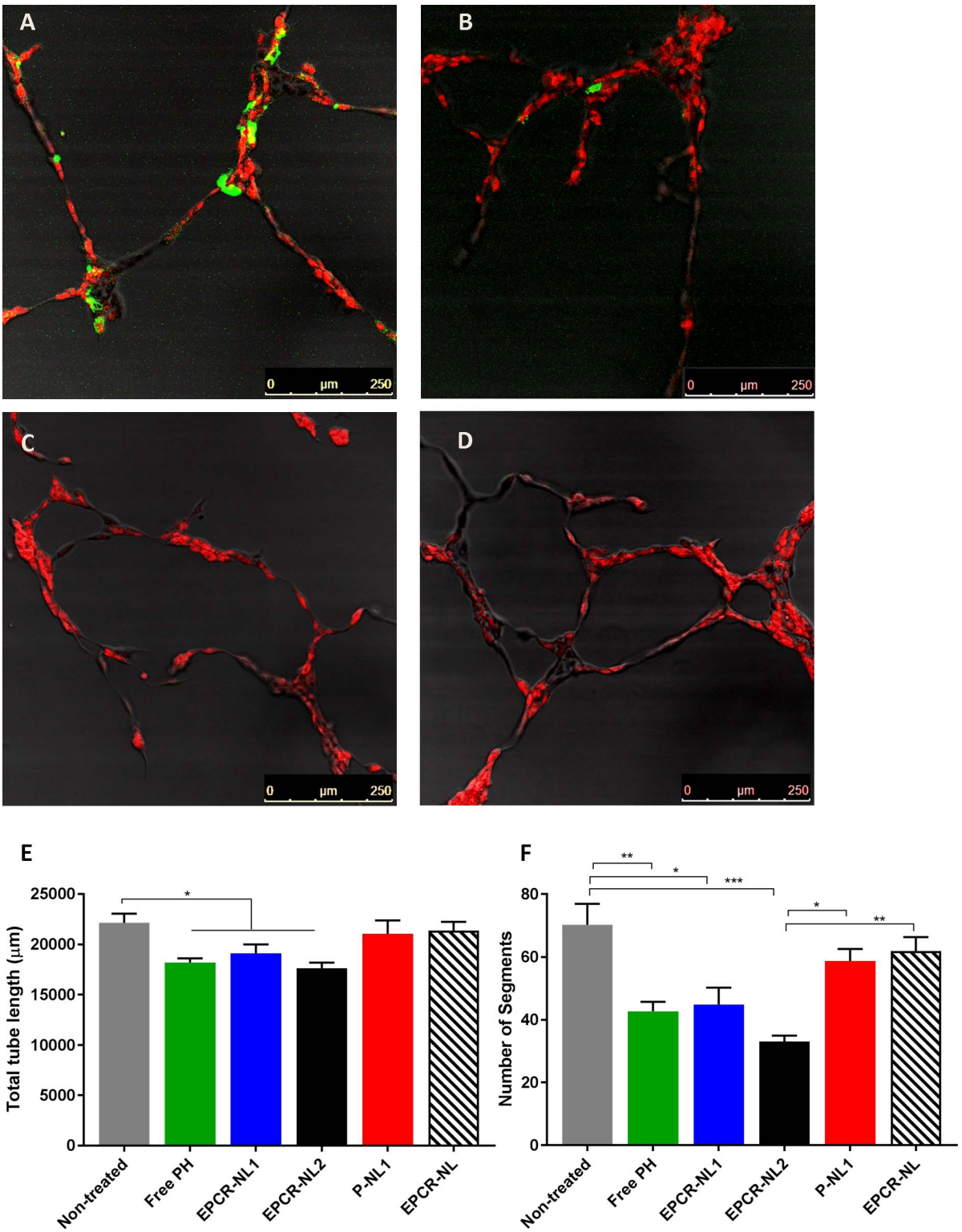

FIGURE 6. Liposome influence on HREC tube formation. (**A**) HRECs incubated with EPCR liposomes, (**B**) HRECs incubated with P-NL liposomes, (**C**) HRECs incubated with B-NL, and (**D**) nontreated cells. Nuclei were stained with TO-PRO-3 and liposomes labeled with Atto 488. *Scale bar*: 250 µm. Quantification of tube formation by assesment of (**E**) the total tubule length and (**F**) and the number of segments 8 hours after seeding the cells on Matrigel matrix. At this timepoint ~4 µM of PH has been released from the liposomes. $^{*}P < 0.05$, $^{**}P < 0.01$, $^{***}P < 0.001$).

45% EE, which is low compared to what has previously been reported (up to 99% EE). However, these high EEs are predominantly associated with large multilamellar liposomes and not small unilamellar liposomes where extrusion results in the structural rearrangement of the liposome bilayer, leading to drug loss.[56] In order to compensate for the loss of corticosteroid, we developed a dual-loaded liposome (EPCR-NL2) to see if this resulted in an improved anti-inflammatory effect.

Cells cultured in high glucose conditions have previously shown to have an inflammatory response.[57–59] Corticosteroids have repeatedly demonstrated inhibition of proinflammatory cytokines in endothelial cells,[58,60–63] and so we compared the effect of prednisolone-loaded EPCR-targeting liposomes (EPCR-NL1 and EPCR-NL2), nontargeting liposomes, and free drug on endothelial cells. The outcome of these studies indicated that EPCR-targeting liposomes and free drug inhibited the secretion of cytokines, with the greatest impact being associated with EPCR-NL2 for both HRECs and HAECs. These findings are in accordance with older studies that have shown that μM concentrations of dexamethasone can induce and approximately 50% decrease in the secretion of IL-6 and a 43% decrease in IL-8 by stimulated endothelial cells,[64,65] whereas cortisol was reported to inhibit IL-6 by approximately 40%.[64] Moreover, the performance of the EPCR-targeting liposomes was superior to nontargeting liposomes, which could be explained by the significantly higher uptake by HRECs and HAECs. Glucocorticoid receptors are found mainly in the cytoplasm[66] and delivering drug payloads into cells should maximize drug-receptor binding. We observed that EPCR-targeting liposomes with significantly lower PH concentrations (~5 μM per day) resulted in similar reductions in IL-6 and IL-8 expression as a single dose of free PH (25 μM). This observation assumes that all the liposomes were endocytosed by cells, which is unlikely. The concentrations of PH released from the liposomes are therefore likely to be lower. Treating stimulated HRECs with a single dose of free PH at 10 μM did not induce any effect in the secretion of IL-6 or IL-8 over 48 hours (see Supplementary Fig. S4). This indicates that it was the continuous intracellular release of PH which lead to an improved effect with a 5-fold lower drug concentration. It has been previously shown that corticosteroids remain active in vitro for several days,[67] can induce cytokine inhibition to stimulated cells within 2 hours of exposure, and retain the effect for up to 48 hours.[64,65] This likely explains the sustained effect observed for free PH. Moreover, EPCR-NL2 exhibited significantly better performance compared to EPCR-NL1 and free drug, which is interesting considering the low concentration of PP (~2.4 μM) and its poor water solubility. PP would have to partition out of the liposomes, either through interactions with proteins and/or phospholipid bilayers in cells and vesicles, before readily reaching glucocorticoid receptors. We did not observe differences in IL-1β secretion levels for any of our culture conditions and treatments, even though it has been previously reported.[58,59]

It has been shown that μM concentrations of triamcinolone acetonide and cortisol as well as nM concentrations of dexamethasone can induce up to a 50% inhibition in endothelial cell tube formation in vitro.[68–70] We observed no inhibition in tube length or the number of segments for HRECs when treated with free PH at 25 μM (data not shown), but did observe inhibition of tube length and segment numbers at 50 μM (Fig. 6). EPCR-NL2 reduced tube length (20% decrease) and significantly reduced the number of segments (50% decrease) 8 hours after seeding HRECs on Matrigel. EPCR-NL1 did not perform as well and was comparable with free PH. No significant differences were observed amongst the EPCR-targeting liposomes and free PH. Based on the PH release profile of EPCR-NL, by the time of our measurements (i.e., 8 hour), less than 8% of the drug had been released from the liposomes, which means that with less than 4 μM of PH, we induced a similar effect as 50 μM of free drug. The nontargeting liposomes that exhibited a similar release profile as the EPCR-targeting liposomes did not induce any effect in cell tube formation. We believe that this enhanced effect occurs because prednisolone is released intracellularly at higher concentrations for EPCR-NL than P-NL, maximizing the probability of drug-glucocorticoid receptor interactions. This results in a lower therapeutic concentration of prednisolone required compared to free prednisolone and a greater effect for EPCR-NL due to the improved endocytosis compared to P-NL. EPCR-NL liposomes showed a more profound effect on the endothelial cell tube formation assay despite the increased complexity of it compared to the two-dimensional cell monolayer assay.

In conclusion, we demonstrated that HRECs strongly express EPCR and that this receptor holds promise as a target for enhanced drug delivery to endothelial cells due to the significant increased uptake of EPCR-targeting liposomes in endothelial cells compared to nontargeting liposomes. EPCR-targeting liposomes showed significant reduction in IL-8 and IL-6 secretion from HRECs and HAECs, as well as suppressed HREC tube length and segment formation. Furthermore, EPCR-targeting liposomes loaded with prednisolone in both the bilayer and aqueous core showed greater anti-inflammatory potential than the equivalent liposomes loaded with prednisolone in the core only or free drug. Further experiments are required to determine if EPCR expression at the retina endothelium is significant in vivo, whether EPCR is evenly distributed or localized in the retina, and whether EPCR can be used as a nanomedicine target in diseased retinas.

Acknowledgments

The authors thank the Core Facility for Integrated Microscopy at the University of Copenhagen for Cryo-TEM support.

Supported by the Velux Foundation, Denmark.

Disclosure: **A. Arta**, None; **A.Z. Eriksen**, None; **F. Melander**, None; **P. Kempen**, None; **M. Larsen**, None; **T.L. Andresen**, None; **A.J. Urquhart**, None

References

1. Lee R, Wong TY, Sabanayagam C. Epidemiology of diabetic retinopathy, diabetic macular edema and related vision loss. *Eye Vis*. 2015;2:17.
2. Sivaprasad S, Gupta B, Crosby-Nwaobi R, Evans J. Prevalence of diabetic retinopathy in various ethnic groups: a worldwide perspective. *Surv Ophthalmol*. 2012;57:347–370.
3. Antonetti DA, Klein R, Gardner TW. Diabetic retinopathy. *N Engl J Med*. 2012;366:1227–1239.
4. Ciulla TA, Amador AG, Zinman B. Diabetic retinopathy and diabetic macular edema: pathophysiology, screening, and novel therapies. *Diabetes Care*. 2003;26:2653–2664.
5. Wan T-T, Li X-F, Sun Y-M, Li Y-B, Su Y. Recent advances in understanding the biochemical and molecular mechanism of diabetic retinopathy. *Biomed Pharmacother*. 2015;74:145–147.
6. Rao LVM, Esmon CT, Pendurthi UR. Endothelial cell protein C receptor: a multiliganded and multifunctional receptor. *Blood*. 2014;124:1553–1562.
7. Ye X, Fukudome K, Tsuneyoshi N, et al. The endothelial cell protein C receptor (EPCR) functions as a primary receptor for protein C activation on endothelial Cells in arteries, veins, and capillaries. *Biochem Biophys Res Commun*. 1999;259:671–677.
8. Moxon CA, Wassmer SC, Milner DA, et al. Loss of endothelial protein C receptors links coagulation and inflammation to parasite sequestration in cerebral malaria in African children. *Blood*. 2013;122:842–851.
9. Li W, Zheng X, Gu J-M, et al. Extraembryonic expression of EPCR is essential for embryonic viability. *Blood*. 2005;106:2716–2722.

10. Crawley JTB, Gu J-M, Ferrell G, Esmon CT. Distribution of endothelial cell protein C/activated protein C receptor (EPCR) during mouse embryo development. *Thromb Haemost*. 2002;88:259–266.
11. Fukudome K, Ye X, Tsuneyoshi N, et al. Activation mechanism of anticoagulant protein C in large blood vessels involving the endothelial cell protein C receptor. *J Exp Med*. 1998;187:1029–1035.
12. Xu J, Qu D, Esmon NL, Esmon CT. Metalloproteolytic release of endothelial cell protein C receptor. *J Biol Chem*. 2000;275:6038–6044.
13. Taylor FB, Stearns-Kurosawa DJ, Kurosawa S, et al. The endothelial cell protein C receptor aids in host defense against *Escherichia coli* sepsis. *Blood*. 2000;95:1680–1686.
14. Laszik Z, Mitro A, Taylor FB, Ferrell G, Esmon CT. Human protein C receptor is present primarily on endothelium of large blood vessels: implications for the control of the protein C pathway. *Circulation*. 1997;96:3633–3640.
15. Sturn DH, Kaneider NC, Feistritzer C, Djanani A, Fukudome K, Wiedermann CJ. Expression and function of the endothelial protein C receptor in human neutrophils. *Blood*. 2003;102:1499–1505.
16. Ebrahim S, Peyman GA, Lee PJ. Applications of liposomes in ophthalmology. *Surv Ophthalmol*. 2005;50:167–182.
17. Pattni BS, Chupin VV, Torchilin VP. New developments in liposomal drug delivery. *Chem Rev*. 2015;115:10938–10966.
18. Bulbake U, Doppalapudi S, Kommineni N, Khan W. Liposomal formulations in clinical use: an updated review. *Pharmaceutics*. 2017;9:12.
19. Peyman GA, Schulman JA, Khoobehi B, Alkan HM, Tawakol ME, Mani H. Toxicity and clearance of a combination of liposome-encapsulated ganciclovir and trifluridine. *Retina*. 1989;9:232–236.
20. Zhang R, He R, Qian J, Guo J, Xue K, Yuan YF. Treatment of experimental autoimmune uveoretinitis with intravitreal injection of tacrolimus (FK506) encapsulated in liposomes. *Invest Ophthalmol Vis Sci*. 2010;51:3575–3582.
21. Goundalkar A, Mezei M. Chemical modification of triamcinolone acetonide to improve liposomal encapsulation. *J Pharm Sci*. 1984;73:834–835.
22. Mastorakos P, Kambhampati SP, Mishra MK, et al. Hydroxyl PAMAM dendrimer-based gene vectors for transgene delivery to human retinal pigment epithelial cells. *Nanoscale*. 2015;7:3845–3856.
23. Duddeck H, Rosenbaum D, Hani M, Elgamal A, Fayez MBE. High-field 1H and 13C NMR spectroscopy of some corticosteroids and related compounds. *Magn Reson Chem*. 1986;24:999–1003.
24. Andresen TL, Davidsen J, Begtrup M, Mouritsen OG, Jørgensen K. Enzymatic release of antitumor ether lipids by specific phospholipase A2 activation of liposome-forming prodrugs. *J Med Chem*. 2004;47:1694–1703.
25. Avnir Y, Ulmansky R, Wasserman V, et al. Amphipathic weak acid glucocorticoid prodrugs remote-loaded into sterically stabilized nanoliposomes evaluated in arthritic rats and in a beagle dog: a novel approach to treating autoimmune arthritis. *Artbritis Rheum*. 2008;58:119–129.
26. Clerc S, Barenholz Y. Loading of amphipathic weak acids into liposomes in response to transmembrane calcium acetate gradients. *Biochim Biophys Acta*. 1995;1240:257–265.
27. Kristensen K, Urquhart AJ, Thormann E, Andresen TL. Binding of human serum albumin to PEGylated liposomes: insights into binding numbers and dynamics by fluorescence correlation spectroscopy. *Nanoscale*. 2016;8:19726–19736.
28. Béduneau A, Saulnier P, Hindré F, Clavreul A, Leroux J-C, Benoit J-P. Design of targeted lipid nanocapsules by conjugation of whole antibodies and antibody Fab' fragments. *Biomaterials*. 2007;28:4978–4990.
29. Janssen APC, Schiffelers R, ten Hagen TL, et al. Peptide-targeted PEG-liposomes in anti-angiogenic therapy. *Int J Pharm*. 2003;254:55–58.
30. Drebert Z, MacAskill M, Doughty-Shenton D, et al. Colon cancer-derived myofibroblasts increase endothelial cell migration by glucocorticoid-sensitive secretion of a pro-migratory factor. *Vascul Pharmacol*. 2017;89:19–30.
31. Dash S, Murthy PN, Nath L, Chowdhury P. Kinetic modeling on drug release from controlled drug delivery systems. *Acta Pol Pharm*.67:217–223.
32. Willcox CR, Pitard V, Netzer S, et al. Cytomegalovirus and tumor stress surveillance by binding of a human γδ T cell antigen receptor to endothelial protein C receptor. *Nat Immunol*. 2012;13:872–879.
33. Anderson M, Omri A. The effect of different lipid components on the in vitro stability and release kinetics of liposome formulations. *Drug Deliv*. 2004;11:33–39.
34. Lian T, Ho RJ. Trends and developments in liposome drug delivery systems. *J Pharm Sci*. 2001;90:667–680.
35. Briuglia ML, Rotella C, McFarlane A, Lamprou DA. Influence of cholesterol on liposome stability and on in vitro drug release. *Drug Deliv Transl Res*. 2015;5:231–242.
36. Kim H, Robinson SB, Csaky KG. Investigating the movement of intravitreal human serum albumin nanoparticles in the vitreous and retina. *Pharm Res*. 2009;26:329–337.
37. Eriksen AZ, Brewer J, Andresen TL, Urquhart AJ. The diffusion dynamics of PEGylated liposomes in the intact vitreous of the ex vivo porcine eye: a fluorescence correlation spectroscopy and biodistribution study. *Int J Pharm*. 2017;522:90–97.
38. Kern TS. Contributions of inflammatory processes to the development of the early stages of diabetic retinopathy. *Exp Diabetes Res*. 2007;2007:1–14.
39. Kowluru RA, Mishra M. Oxidative stress, mitochondrial damage and diabetic retinopathy. *Biochim Biophys Acta*. 2015;1852:2474–2483.
40. Wang H, Feng L, Hu JW, Xie CL, Wang F. Characterisation of the vitreous proteome in proliferative diabetic retinopathy. *Proteome Sci*. 2012;10:15.
41. Lee WJ, Kang MH, Seong M, Cho HY. Comparison of aqueous concentrations of angiogenic and inflammatory cytokines in diabetic macular oedema and macular oedema due to branch retinal vein occlusion. *Br J Ophthalmol*. 2012;96:1426–1430.
42. Elner SG, Elner VM, Jaffe GJ, Stuart A, Kunkel SL, Strieter RM. Cytokines in proliferative diabetic retinopathy and proliferative vitreoretinopathy. *Curr Eye Res*. 1995;14:1045–1053.
43. Abcouwer SF. Angiogenic factors and cytokines in diabetic retinopathy. *J Clin Cell Immunol*. 2013;1:1–23.
44. Ford JA, Lois N, Royle P, Clar C, Shyangdan D, Waugh N. Current treatments in diabetic macular oedema: systematic review and meta-analysis. *BMJ Open*. 2013;3:e002269.
45. Campos EJ, Campos A, Martins J, Ambrósio AF. Opening eyes to nanomedicine: where we are, challenges and expectations on nanotherapy for diabetic retinopathy. *Nanomedicine*. 2017;13:2101–2113.
46. Smoak KA, Cidlowski JA. Mechanisms of glucocorticoid receptor signaling during inflammation. *Mech Ageing Dev*. 2004;125:697–706.
47. Itakura H, Akiyama H, Hagimura N, et al. Triamcinolone acetonide suppresses interleukin-1 beta-mediated increase in vascular endothelial growth factor expression in cultured rat Müller cells. *Graefes Arch Clin Exp Ophthalmol*. 2006;244:226–231.
48. Nauck M, Roth M, Tamm M, et al. Induction of vascular endothelial growth factor by platelet-activating factor and platelet-derived growth factor is downregulated by corticosteroids. *Am J Respir Cell Mol Biol*. 1997;16:398–406.

Investigative Ophthalmology & Visual Science

49. Prabhala P, Bunge K, Ge Q, Ammit AJ. Corticosteroid-induced MKP-1 represses pro-inflammatory cytokine secretion by enhancing activity of tristetraprolin (TTP) in ASM cells. *J Cell Physiol*. 2016;231:2153–2158.
50. Schmidt J, Metselaar JM, Wauben MHM, Toyka KV, Storm G, Gold R. Drug targeting by long-circulating liposomal glucocorticosteroids increases therapeutic efficacy in a model of multiple sclerosis. *Brain*. 2003;126:1895–1904.
51. Piel G, Piette M, Barillaro V, Castagne D, Evrard B, Delattre L. Betamethasone-in-cyclodextrin-in-liposome: the effect of cyclodextrins on encapsulation efficiency and release kinetics. *Int J Pharm*. 2006;312:75–82.
52. Avnir Y, Turjeman K, Tulchinsky D, et al. Fabrication principles and their contribution to the superior in vivo therapeutic efficacy of nano-liposomes remote loaded with glucocorticoids. *PLoS One*. 2011;6:e25721.
53. Shaw IH, Knight CG, Dingle JT. Liposomal retention of a modified anti-inflammatory steroid. *Biochem J*. 1976;158:473–476.
54. Teshima M, Kawakami S, Nishida K, et al. Prednisolone retention in integrated liposomes by chemical approach and pharmaceutical approach. *J Control Release*. 2004;97:211–218.
55. Wijagkanalan W, Higuchi Y, Kawakami S, Teshima M, Sasaki H, Hashida M. Enhanced anti-inflammation of inhaled dexamethasone palmitate using mannosylated liposomes in an endotoxin-induced lung inflammation model. *Mol Pharmacol*. 2008;74:1183–1192.
56. Bhardwaj U, Burgess DJ. Physicochemical properties of extruded and non-extruded liposomes containing the hydrophobic drug dexamethasone. *Int J Pharm*. 2010;388:181–189.
57. Liu T, Gong J, Chen Y, Jiang S. Periodic vs. constant high glucose in inducing pro-inflammatory cytokine expression in human coronary artery endothelial cells. *Inflamm Res*. 2013;62:697–701.
58. Liu Y, Costa M, Gerhardinger C. IL-1β is upregulated in the diabetic retina and retinal vessels: cell-specific effect of high glucose and IL-1β autostimulation. *PLoS One*. 2012;7:1–8.
59. Li Y, Bharath LP, Qian Y, et al. γ-Carboxyethyl hydroxychroman, a metabolite of γ-tocopherol, preserves nitric oxide bioavailability in endothelial cells challenged with high glucose. *Exp Biol Med*. 2016;241:2056–2062.
60. Urakaze M, Temaru R, Satou A, Yamazaki K, Hamazaki T, Kobayashi M. The IL-8 production in endothelial cells is stimulated by high glucose. *Horm Metab Res*. 1996;28:400–401.
61. Shen H, Rong H. Pterostilbene impact on retinal endothelial cells under high glucose environment. *Int J Clin Exp Pathol*. 2015;8:12589–12594.
62. Heimbürger M, Lärfars G, Bratt J. Prednisolone inhibits cytokine-induced adhesive and cytotoxic interactions between endothelial cells and neutrophils in vitro. *Clin Exp Immunol*. 2000;119:441–448.
63. Ding Y, Gao Z-G, Jacobson KA, Suffredini AF. Dexamethasone enhances ATP-induced inflammatory responses in endothelial cells. *J Pharmacol Exp Ther*. 2010;335:693–702.
64. Waage A, Slupphaug G, Shalaby R. Glucocorticoids inhibit the production of IL6 from monocytes, endothelial cells and fibroblasts. *Eur J Immunol*. 1990;20:2439–2443.
65. Nyhlén K, Linden M, Andersson R, Uppugunduri S. Corticosteroids and interferons inhibit cytokine-induced production of IL-8 by human endothelial cells. *Cytokine*. 2000;12:355–360.
66. Vandevyver S, Dejager L, Libert C. On the trail of the glucocorticoid receptor: into the nucleus and back. *Traffic*. 2012;13:364–374.
67. Bindreither D, Ecker S, Gschirr B, Kofler A, Kofler R, Rainer J. The synthetic glucocorticoids prednisolone and dexamethasone regulate the same genes in acute lymphoblastic leukemia cells. *BMC Genomics*. 2014;15:1–8.
68. Small GR, Hadoke PWF, Sharif I, et al. Preventing local regeneration of glucocorticoids by 11beta-hydroxysteroid dehydrogenase type 1 enhances angiogenesis. *Proc Natl Acad Sci U S A*. 2005;102:12165–12170.
69. Matsuda S, Gomi F, Oshima Y, Tohyama M, Tano Y. Vascular endothelial growth factor reduced and connective tissue growth factor induced by triamcinolone in ARPE19 cells under oxidative stress. *Invest Ophthalmol Vis Sci*. 2005;46:1062–1068.
70. Logie JJ, Ali S, Marshall KM, Heck MMS, Walker BR, Hadoke PWF. Glucocorticoid-mediated inhibition of angiogenic changes in human endothelial cells is not caused by reductions in cell proliferation or migration. *PLoS One*. 2010;5:e14476.

Investigative Ophthalmology & Visual Science